Partial Discharge Inception Voltage: Precise and Robust Numerical Estimation Based on Extensive Dielectric Spectroscopy Measurements

Youcef Kemari, Guillaume Belijar, Lionel Laudebat, Sombel Diaham, Zarel Valdez-Nava

Partial Discharge Inception Voltage: Precise and Robust Numerical Estimation Based on Extensive Dielectric Spectroscopy Measurements

Youcef KEMARI
Greener Technologies - IRT Saint Exupery
LAPLACE
Université de Toulouse, CNRS, INPT, UPS
Toulouse, France
youcef.kemari@irt-saintexupery.com
kemari@laplace.univ-tlse.fr

Guillaume BELIJAR
Greener Technologies
IRT Saint Exupery
Toulouse, France
guillaume.belijar@irt-saintexupery.com

Lionel LAUDEBAT
LAPLACE
Université de Toulouse, CNRS, INPT, UPS
Toulouse, France
laudebat@laplace.univ-tlse.fr

Sombel DIAHAM
LAPLACE
Université de Toulouse, CNRS, INPT, UPS
Toulouse, France
sombel.diaham@laplace.univ-tlse.fr

Zarel VALDEZ-NAVA
LAPLACE
Université de Toulouse, CNRS, INPT, UPS
Toulouse, France
valdez@laplace.univ-tlse.fr

***Abstract*— This paper provides a robust experimental-simulation approach in predicting the Partial discharge inception voltage (PDIV) for aeronautical applications. First, two polymers used as insulators in aeronautic components have been selected in this work, a polyimide and a polyetheretherketone. To study the electrical behavior of these materials, extensive dielectric spectroscopy measurements are carried out for different electric fields, temperatures and frequencies (E, T, *and f*). Then, a needle-plane configuration is adopted for PDIV modeling using finite-element method (FEM). As the model is strongly dependent upon the accurate estimation of the electric field, dielectric characterizations results are integrated in simulations to improve the precision of calculations. Thereafter, the PDIV can be estimated with the aid of Townsend's theory. Finally, a comparison between measured and computed PDIV values is presented and discussed.**

Keywords— partial discharges, PDIV, dielectric spectroscopy, modeling, aeronautical environment

I. Introduction

With the concept of "More Electrical Aircraft", substantial efforts are being paid on increasing the voltage in the onboard systems. For instance, in the Airbus A350, a 230/400 VAC system has been adopted [1]. To enable hybrid propulsion or full-electric aircraft, even higher voltage will be required to maintain high power density. However, high electric fields combined with high operating temperatures and with low ambient pressure will increase the risk of PD occurrence in aeronautical cables and connectors [2].

On the other hand, experimental measurement of PD is not trivial to be performed in every test configuration and does not always provide sufficient information about the location of the discharge. Thus, a lot of work is still needed to make significant progress in PD modeling and prediction [3]. Moreover, dielectric properties of insulating materials can impact the distribution of the electric field and thus, the occurrence of the PD. These material properties strongly depend on temperature, frequency and also on the electric field magnitude itself.

In the framework of HYBELEC project at IRT Saint Exupéry, the case study considered in this paper for PDIV calculations and measurements consists in an insulating film deposited between a needle and a flat electrode. Two materials used in standard aeronautical components are chosen here; a polyimide (PI/FEP) and a polyetheretherketone (PEEK), to examine the proposed PDIV estimation approach.

Also, it can be found in many models existing in the literature that the dielectric constant ε_r' and the conductivity σ_{AC} are generally defined from suppliers datasheets and their variations with temperature, frequency and electric field are not always considered [3-5]. In some cases, this can affect the accuracy of the electric field calculation and thus, the estimation of PDIV. This could lead to suboptimal insulation system and overweight or unreliability. In light of this, this study puts forth the investigation of material properties impact on electric field distribution and PDIV by proposing an extensive measurements of polymers dielectric properties under different constraints (E, T, and *f*). According to the literature, high AC voltage dielectric spectroscopy measurements up to 1414 V_{rms} have never been carried out on the studied materials here few times before. The obtained data are then used through a numerical model based on for precise PDIV estimation at 50 Hz. Also, simulated and experimental results are compared.

II. Procedure

A. Materials

The studied polyimide material, under the trade name Kapton FN®, is intended for aeronautic cables manufacturing. The polyimide, was provided in the form of tapes with a thickness of 30 µm. It consists of 25 µm of pure polyimide (Kapton HN® type) covered on each side by 2.5 µm of Fluorinated ethylene propylene (FEP) layer. Besides, PEEK

circular shaped samples were provided with a thickness of 400 µm and a diameter of 30 mm. This material is used in different aeronautical connectors.

B. High voltage-frequency domain dielectric spectroscopy

A broadband dielectric analyzer (Novocontrol Alpha-A, Montabaur, Germany) was used for ε_r' and σ_{AC} measurements from 20 °C up to the maximum rated temperature (260 and 200 °C for PI and PEEK respectively). Measurements were performed thanks to a high voltage amplifier (Novocontrol HVB-4000, Montabaur, Germany) that allows to apply voltage up to 1414 V_{rms} in the frequency range from 1 to 10^3 Hz. Also, all samples are metallized by sputtering on both sides with 30 nm-thick gold layer of diameter 10 mm to ensure perfect electric contact. Prior to measurements, samples were dried in an oven at 150 °C for 48 h.

C. PDIV measurements

In aeronautical components, partial discharges may occur in defects or air-filled voids or gaps between high voltage conductors and the insulation material. To simulate such a structure and the PD process, we adopted a needle-plane configuration in the experiment with the tip of the needle in contact with the sample. The schematic diagram of the experimental setup for PD measurements under AC voltages is shown in Fig.1.

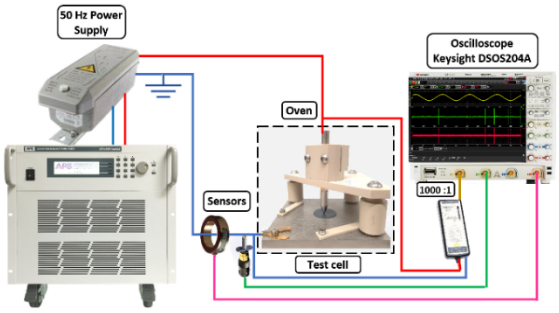

Fig. 1. Schematic diagram of the PD experimental setup.

After being dried, the samples were mounted in an in-house made test cell between a needle electrode, with an edge curvature radius of 1 mm, and a grounded flat electrode. Also, a 30 nm-thick gold layer was deposited on the other side of the sample in order to ensure the absence of air layer between the ground and the sample. After, the test cell was placed in an oven that can span from room temperature to 210 °C which corresponds to the maximum operating temperature of the test cell.

The 50 Hz high voltage was applied to the needle by a PD free test transformer (delivering up to 5 kV_{peak} and a maximum of 100 mA_{rms}) associated to an AC power source (CFS330 Adaptive Power Systems, Taiwan). For PD detection, two non-intrusive sensors were placed on the cable connected between the test cell and the ground: a Jack-SMA connector with a capacitive effect and a wideband fast current transformer (Bergoz FCT-016-1.25, France). The acquisition tool used is an oscilloscope (Keysight DSOS204A, France) with a sampling rate of 20 GSa/s and numerical bandwidth of 2 GHz. All PDIV measurements were performed in peak detect mode with frequency sampling fixed at 5 GS/s. PDIV values were measured 5 times at each temperature for both materials.

D. Electric field simulation

The same needle-plane configuration considered in this paper for PD experiments was analyzed by FEM with the aid of COMSOL Multiphysics® (5.5). We used the AC/DC module (Electric current) to compute the potential and the electric field lines. First, the electrode geometry was extracted from the real object and then drawn with the insulation material and the flat grounded electrode as shown in Fig. 2. Due to the symmetry of this configuration, it can be also modeled in a 2D-axisymetrical format. Thereafter, the entire domain has been discretized during the mesh process into triangle type finite elements of size between 0.5 and 20 µm. To increase the number of elements and thus to improve the precision of the solution, a refinement of the mesh, as shown in Fig. 3, has been implemented in the region of great interest where PDs firstly ignite. Dielectric properties of the studied PI/FEP and PEEK were successfully defined by interpolating values obtained from dielectric measurements. Whereas ε_r' and σ_{AC} of air are considered unchanged with the modification of temperature (1 and 10^{-16} $S.m^{-1}$ respectively).

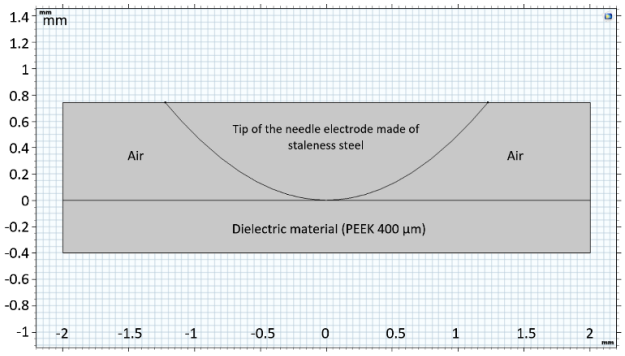

Fig. 2. Geometry of the needle-plane model.

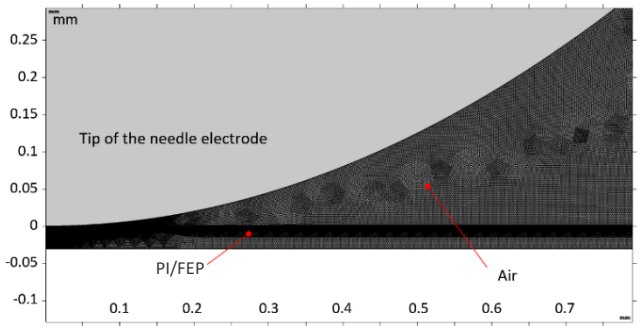

Fig. 3. Meshing strategy represented in the 2D-axisymetrical format.

E. AIRLIFT

PDIV has been computed thanks to a specific numerical software named "pArtial dIscharge Risk evaLuatIon soFTware" (AIRLIFT). AIRLIFT is based on Paschen's law established from Townsend's theory in air between electrodes. Paschen's law gives the voltage V_b corresponding to the initiation of the PD in gases between parallel conducting plates as [5]:

$$V_b = \frac{B.p.d}{C + ln(p.d)}; \quad with \quad C = ln\left(\frac{A}{ln\left(1+\frac{1}{\gamma}\right)}\right) \qquad (1)$$

where p is the gas pressure in Torr, d is the distance in cm, A and B are the coefficients that depend on the considered gas and temperature and γ is the Townsend's secondary emission coefficient. The previous parameters were set from literature as: A = 15 (Torr.cm)$^{-1}$, B = 365 V. (Torr.cm)$^{-1}$ [2] and γ = 4.8x10^{-4} [6]. For a given set of environmental parameters, the computed electric potential is used to estimate PDIV. In the current work, PD measurements and simulations are performed at the atmospheric pressure (1,013 bar).

III. Results and Discussions

A. Dielectric Spectroscopy Results

We present in Fig. 4 the variations of the dielectric constant ε_r' and the AC conductivity σ_{AC} of PI/FEP versus frequency and electric field at different temperatures. For temperatures below 210 °C, no significant change in the two properties was observed as a function of temperature. Besides, Fig.4 (b) shows the quasi-linear evolution of the conductivity as a function of frequency following a slope close to unity. This last result indicates that the dielectric behavior of the PI/FEP is mainly related to the mechanism of dipolar polarization [7]. On the other hand, we can observe that both properties are affected by the increase of the electric field at all temperatures. This effect is more noticeable in σ_{AC} curves as shown in Fig. 4(b).

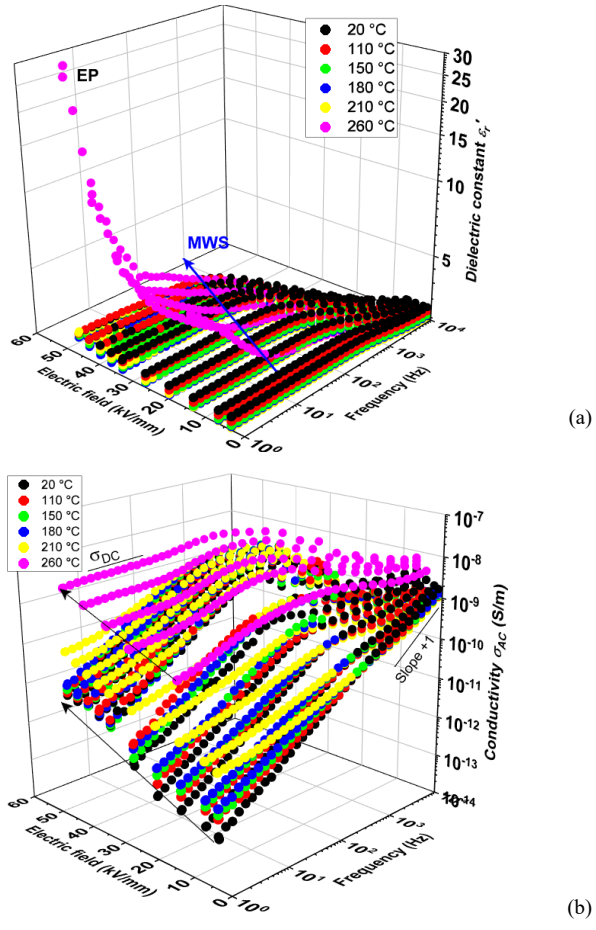

Fig. 4. (a) Dielectric constant and (b) AC conductivity of PI/FEP as a function of electric field, temperature and frequency.

In addition, the curves of the conductivity as a function of the frequency deviate at 210 °C towards a form of a horizontal plateau at low frequencies. This can be referred to the displacement of charge carriers at the interfaces within the bulk of the polyimide (interfacial or Maxwell-Wagner-Sillars (MWS) polarization phenomenon). In fact, MWS polarization is generally characterized by a slight increase in permittivity ($\Delta\varepsilon'_r$ <0.3) [7].

As the MWS phenomenon is thermally activated, we can observe the progressive shift of ε_r' and σ_{AC} towards higher frequencies as the temperature increases to 260 °C. At this high temperature, we observe clearly a drastic increase in the permittivity ($\Delta\varepsilon'_r$ >10) at low frequencies accompanied by a very significant increase in the conductivity which becomes frequency independent (slope of 0). These evolutions represent the electrical signature of the polarization at the electrodes (EP) also reported in the literature for polyimides [7, 8]. This phenomena results from the accumulation of thermally excited charge carriers in the vicinity of the polymer/electrode interface.

Moreover, we observe that the curves of ε_r' and σ_{AC} are shifted towards higher frequencies when the applied field increases at 260 °C as indicated by blue arrow in Fig.4 (a). Hence, it is important to point out that EP phenomenon can be also electrically activated by high electric field values (>32 kV.mm^{-1}) when the temperature is sufficiently high as found in this study. In other words, the mobile charge carriers have more energy to move rapidly toward the vicinity of the electrodes under enhanced electric fields.

As far as PEEK is concerned, Fig. 5 shows the evolution of ε_r' and σ_{AC} versus the different measuring parameters (E, T, *and f*). We found that the obtained permittivity values are relatively high compared to those reported elsewhere (3.1< ε_r'<4.5) [9]. This can be attributed to the process of the chemical synthesis of PEEK and to the nature of fillers injected into the polymer matrix [9].

Given the thickness of the samples (400 µm), the applied electric field here remains relatively low (maximum value of 3.3 kV.mm^{-1}). Consequently, no significant impact of the electric field has been found here on PEEK properties. However, we can clearly distinguish the influence of temperatures higher than 150 °C which corresponds practically to the glass transition temperature. Below 150 °C, the dielectric behavior of PEEK as a function of frequency is typical involving a linear increasing of the conductivity and a quasi-constant permittivity attributed to the to the efficient rotation of highly polar side groups such as COOH and SO_2 [9].

On the other hand, ε_r' and σ_{AC} begin to increase at low frequencies at 150 °C. The origin of this evolution is probably attributable to an intrinsic MWS interfacial polarization. This increase with temperature continues up to 200 °C where we can notice a variation in permittivity $\Delta\varepsilon_r'$ > 1 (+15 to 30 % of values obtained at 20 °C, depending on the frequency) and an increase in conductivity of half a decade with respect to that measured at 20 °C. In addition, plateau region independent of frequency start to appear above 150 °C at low frequencies indicating the activation of DC conduction.

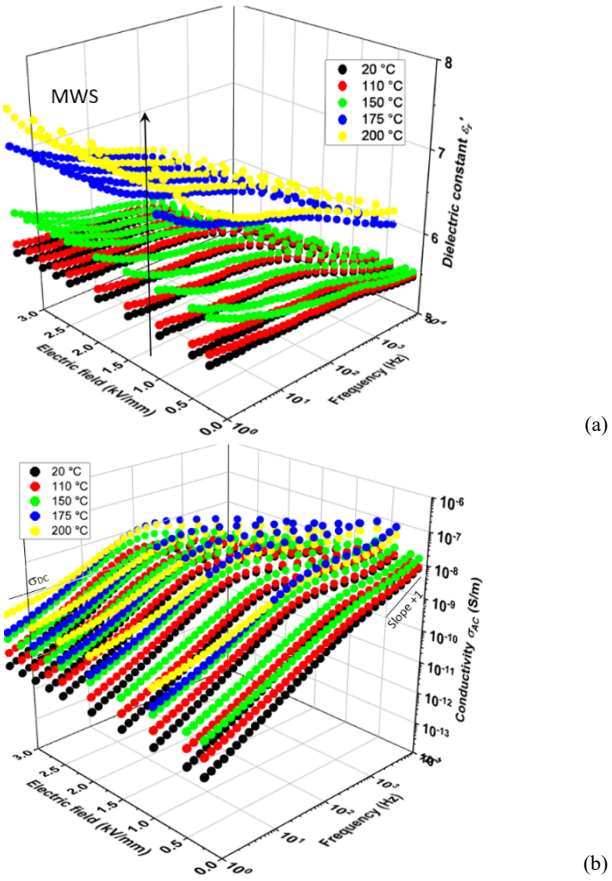

Fig. 5. (a) Dielectric constant and (b) AC conductivity of PEEK as a function of electric field, temperature and frequency.

B. *Electric Field Computation Results*

At atmospheric pressure of 1 bar (750 Torr), the Paschen's minimum for air is about 325 V_{peak} for a distance of about 10 µm (pressure-distance product of 0.75 Torr.cm) [2]. For this reason, we are interested in the area where air gaps between the needle and the material have values at the same order of magnitude that the Paschen's minimum. In this section, Fig. 6 and 7 present the distribution of the computed electric field in the case of PI/FEP and PEEK respectively as the temperature changes.

Contour plots with 9 levels are used for better visualization of the electric field changes. Indeed, contour plots display the maximum electric field results on a series of colored regions where each contour interface indicates a surface where the stress is at a constant level (specified by the color legend in $V.m^{-1}$). For the simulation, an electric potential of 700 V_{peak} at 50 Hz was applied on the needle electrode. Comparing the temperature dependence of the dielectric response of both materials (Fig.4 and 5) with results shown is Fig.6 and 7, the changing of the electric field distribution with temperature can be assigned to the significant changes of the insulation properties. It seems that the electric field in the polyimide bulk becomes more localized in the vicinity of the needle tip as the temperature rises (as indicated by the blue arrow). Besides, the enlargement of the red region (as highlighted by the red arrow in Fig. 6 and 7) implies the enhancement of the electric field in the air and thus the acceleration of free electrons. Consequently, PDIV becomes lower for the same field line length.

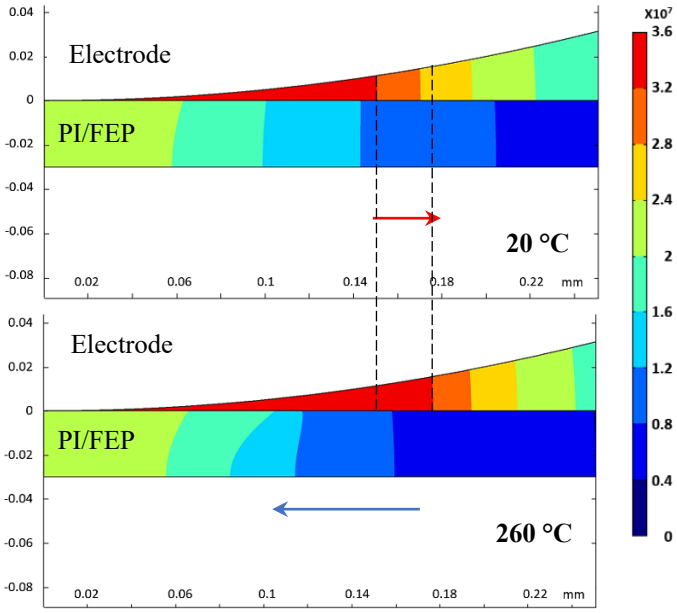

Fig. 6. Contour plot of the electric field in needle-PI/FEP case study under a 50 Hz voltage of 700 V_{max} : comparaison between 20 and 260 °C results.

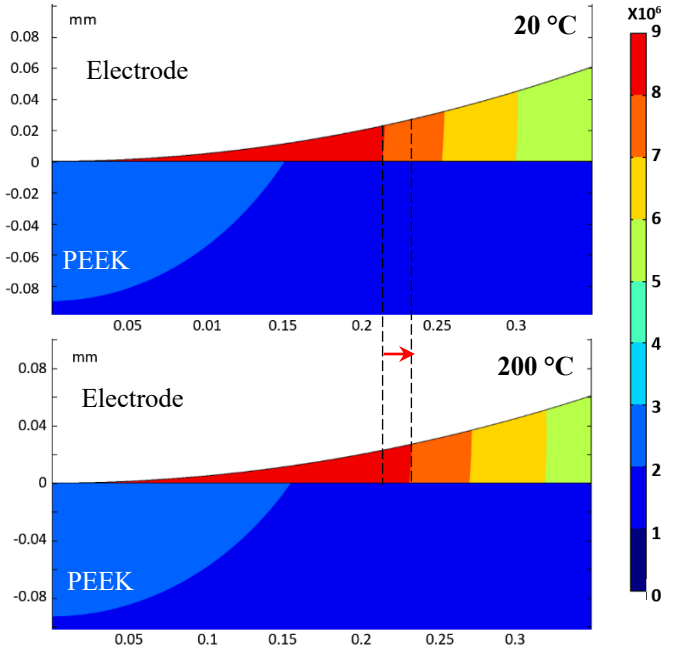

Fig. 7. Contour plot of the electric field in needle-PEEK case study under a 50 Hz voltage of 700 V_{max} : comparaison between 20 and 200 °C results.

C. *Comparaison Between Experiments and Simulations*

This section provides a comparison between experimental PDIV values and those obtained with numerical models. The first model (Model A) is based on extensive dielectric measurements on PI/FEP and PEEK. A second model (Model B) was implemented for the same geometry by defining dielectric properties as given in suppliers' datasheet (Table I). The PDIV values obtained by both models are plotted as a function of the temperature and compared with experimental results as shown in Fig. 8.

TABLE I. MATERIALS PROPERTIES GIVEN IN DATASHEETS

Material	Dielectric constant	Conductivity (S.m^{-1})
PI/FEP	3.1	3.5 x 10^{-12}
PEEK	3.9 at 1 MHz	2.8 x 10^{-12}

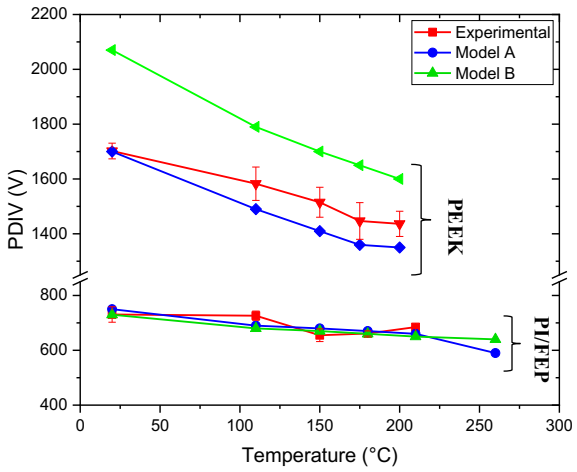

Fig. 8. PDIV variation with temperature and comparaison between Model A, Model B and experiments.

In the case of PI/FEP material, a great agreement is found between computed and measured PDIV. The maximum deviations between average experimental and computed PDIV can be found in Table II. It can be seen that the deviation with experiments are slightly lower in the Model A based on dielectric measurements. Besides, results found by both models A and B are practically similar up to 210 °C, which is in agreement with dielectric measurements results shown in Fig. 4. In fact, we have found that PI/FEP properties changes under 50 Hz are not significant with temperatures up to 210 °C. Also, the drastic variations of ε_r' and σ_{AC} were assessed above this temperature essentially at low frequencies.

On the other hand, the simulated PDIV of Model A is kept with a variation below 6.9 % compared to experimental values in the case of PEEK. Moreover, the computed PDIV values in this Model are always found below measured ones, close to the minimum experimental values. However, the predicted results with Model B (based on values given in Table I) are significantly higher than measured ones. This can be explained by the important difference between dielectric characterizations values presented in this work and those can be extracted from the literature and datasheets.

TABLE II. MAXIMAUM ERROR BETWEEN EXPERIMENTAL AND COMPUTED PDIV VALUES

Material	Model A	Model B
PI/FEP	5 %	6.4 %
PEEK	6.9 %	21.6 %

IV. CONCLUSION

This work presents a robust numerical estimation of PDIV for aeronautical applications using FEM models linked with a numerical solver. The proposed approach is based on HV dielectric spectroscopy characterizations under various voltages, temperatures and frequencies on PI/FEP and PEEK. Spectroscopy results show that dielectric properties of PI/FEP are significantly affected at 260 °C where a conduction process and space charge accumulations in the vicinity of electrodes occur simultaneously with a large effect on the dielectric response. It has been found that this process can be enhanced as well by high electric field values. Concerning PEEK material, properties changes begin to take place in the temperature range from 150 to 200 °C, mainly due to intrinsic MWS interfacial polarization process. The integration of those results in our model led us to obtain more precise predictions of PDIV as a function of temperature for a needle-plane configuration compared to a second model based on fixed values extracted from the literature or datasheets.

The approach presented in this work can be the groundwork to study more complex geometries of real aeronautical components such as cables and connectors with multiple materials. Also, the changes of dielectric properties at high temperature, eventually under HV, could modify the electric field distribution in the component leading to more PD risks.

ACKNOWLEDGMENT

This work has been carried out in the framework of HYBELEC project at IRT Saint Exupéry with the financial support of the French Agence Nationale de la Recherche (ANR), Safran SEP, Airbus, Nexans and Souriau. The authors would like to thank Patrick RYBSKI (Nexans), Kossi BAYODA (Souriau), Thomas HÄHNER (Nexans), and Alain PHILIPPE (Souriau) for the provision of study materials and associated data.

REFERENCES

[1] T. Billard, C. Abadie, and B. Taghia, “Non-Intrusive Partial Discharges Investigations on Aeronautic Motors,” SAE Technical Paper 2016-01-2058, p.18, September 2016.

[2] E. Sili, J. P. Cambronne, N. Naude and R. Khazaka, “Polyimide lifetime under partial discharge aging: effects of temperature, pressure and humidity,” in IEEE Trans. Dielectr. Electr. Insul, vol. 20, no. 2, pp. 435-442, April 2013.

[3] C. Van de Steen, C. Abadie and G. Belijar, “Partial discharge detection, Experimental-Simulation Comparison and actual limits,” 2020 IEEE Electrical Insulation Conference (EIC), Knoxville, TN, USA, 2020, pp. 537-541.

[4] S. Pin, G. Belijar, L. Fetouhi, L. Somer, C. Van de Steen and L. Albert, “Ageing study in aircraft electromechanical chain: systems modeling for property evolution monitoring,” 2020 IEEE Electrical Insulation Conference (EIC), Knoxville, TN, USA, 2020, pp. 79-84.

[5] G. Parent, M. Rossi, S. Duchesne and P. Dular, “Determination of Partial Discharge Inception Voltage and Location of Partial Discharges by Means of Paschen’s Theory and FEM,” in IEEE Trans. on Magn, vol. 55, no. 6, pp. 1-4, June 2019.

[6] P. Collin, D. Malec and Y. Lefevre, "About the relevance of using Paschen's criterion for partial discharges inception voltage (PDIV) estimation when designing the electrical insulation system of inverter fed motors," 2019 IEEE Electrical Insulation Conference (EIC), Calgary, AB, Canada, 2019, pp. 513-516.

[7] R. Khazaka, M.-L. Locatelli, S. Diaham, P. Bidan, L. Dupuy and G. Grosset, "Broadband dielectric spectroscopy of BPDA/ODA polyimide films", J. Phys. D: Appl. Phys., vol. 46, pp. 065501, 2013.

[8] S. Diaham and M-L. Locatelli, "Dielectric properties of polyamide-imide", J. Phys. D: Appl. Phys., vol. 46, pp. 185-302, 2013.

[9] J.Wei, T.Ju, W. Huang, J. Song, N. Yan, F. Wang, A. Shen, Z. Li and L. Zhu, “High dielectric constant dipolar glass polymer based on sulfonylated poly(ether ether ketone),” Polymer, vol. 178, 121688, 2019.